Academy of Sciences, USSR

SPACE RESEARCH INSTITUTE

D-251

M.I.Verigin, K.I.Gringauz, T.Gombosi, T.K.Breus,
V.V.Bezrukikh, A.P.Remizov, G.I.Volkov

PLASMA NEAR VENUS FROM THE VENERA-9 AND 10 WIDE-ANGLE ANALYZER DATA

To be presented to Symposium on Solar Wind Interaction with Venus (SIV3) IAGA Assembly, Seattle, August 1977

Moscow

ACADEMY OF SCIENCE OF THE USSR

SPACE RESEARCH INSTITUTE

D-251

M.I.Verigin, K.I.Gringauz, T.Gombosi, T.K.Breus,
V.V.Bezrukikh, A.P.Remizov, G.I.Volkov

PLASMA NEAR VENUS FROM THE VENERA-9 AND 10 WIDE-ANGLE ANALYZER DATA

To be presented to Symposium on Solar
Wind Interaction with Venus (SIV3) IAGA
Assembly, Seattle, August 1977

1977

I. Introduction

Venera-9 and Venera-10 spacecrafts were launched to Venera satellites orbits on October 22 and October 25, 1975, respectively. The period of the satellites was ~ 48 hours, their orbits were ~ 1500 km high in pericenter and ~ 110000 km in apocenter, their inclination was ~ 30°.

Experiments with wide-angle plasma analyzers described below were the first simultaneous measurements of both electron and ion plasma components near Venus. Plasma experiments on Venera-4 [1] , Mariner 5 [2] and Venera 6 [3] measured only an ion component, while Mariner 10 [4] measured only an electron component of plasma. Until Venera-9 and Venera-10 flights, no experimental data were available on plasma characteristics in the planet optical umbra. An ion plasma component was measured on-board Venera-9 and 10 spacecrsft in 16 energy intervals within the energy range 0 to 4400 eV with a modulation analyzer (a Faraday cup). It had an angular pattern $\pm 45°$ and was sunward oriented. An electron plasma component was measured with a wide-angle ($\pm 40°$) anti-sunward oriented analyzer. Electron energy distribution was analyzed by the retarding potential method. 16 values of retarding potential U_R were used in the range $0 \leq U_R \leq 300$ V. The equipment used slightly differed (sensors

were the same) from that used in near-Mars plasma experiments made on-board Mars 2, Mars 3, Mars 5 and described in more detail elsewhere [5] .

In all near-planet measurement sessions analyzed (but for that on April 19, 1976) electron and ion analyzer currents were recorded once per second. Ten current measurements were made in each energy interval and for each U_R-value, so that the complete differential ion and integrated electron energy spectra were measured in 160 s. On April 19, 1976 currents were measured once each 4 seconds, one measurement was made in each energy interval and for each U_R value. An interval between the two spectra measurements was 56 seconds. Venera-9 satellite measured simultaneously both electron and ion plasma components. Satellite Venera-10 measured an electron plasma component only because of some malfunctioning as was mentioned in [6,7] however, on April 19, 1976 ion plasma component measurements resumed; their data are used below.

The paper of the research team who are engaged in experiment program for Pioneer-Venus 1978 satellite [8] formulated a series of questions about the properties of near-Venus space which should be answered. The results of Venera-9 and Venera 10 plasma measurements yield answers to some of these questions.

The amount of experimental data obtained by both satellites is large; not all of it has been processed up to June 1977, hence this publication is not a final one.

II. Typical features of Near-Venus bow shock

Time resolution of Venera-9 and Venera-10 instruments allows sufficiently detailed study of electron and ion plasma compo-

nents when traversing the near-planet bow shock. Considerably different front structure were observed along different orbits of the satellites when they traversed the bow shock. Fig.1 gives the results of measurements of the ion and electron plasma components and the magnetic field, carried out on Venera-9 satellite in 50 seconds from the near planet bow shock on December 17, November 1 and October 26, 1975 (these and below given magnetic data have been kindly supplied to us by Sh.Dolginov and E.Yeroshenko). The same Figure shows mean ion energy values E_i in the energy intervals where measurements were made near the bow shock as well as retarding potentials U_R of the electron analyzer. As Figure 1 demonstrates, the intersection of the bow shock, S, within the telemetry time resolution is simultaneously recorded from ion and electron plasma component measurements and from magnetic field measurements. It was observed $\lesssim 1$ s on December 17, about 15 to 20 s on November 1, and the bow shock was crossed at least three times during observations October 26. If it is assumed that the bow shock did not move on November 1 and October 26, then, with a satellite velocity v of about 7 km·s^{-1} taken into account, its thickness can be calculated as $\lesssim 10$ km and about 100 to 150 km, respectively. The first and the third interactions of the bow shock on October 26, 1975 took $\tau \sim 2$ s while for the second T was about 4 sec. Under the assumption that in the first case the velocities of the bow shock motion, V, and of the satellite, v, were oppositely directed, while in the second case they were in one direction, the bow shock velocity and its thickness δ can be assessed for October 26, respectively, as $V = v(T+\tau)(T-\tau)^{-1} \approx 20$ km·s and $\delta = (V+v)\tau \approx 60$ km.

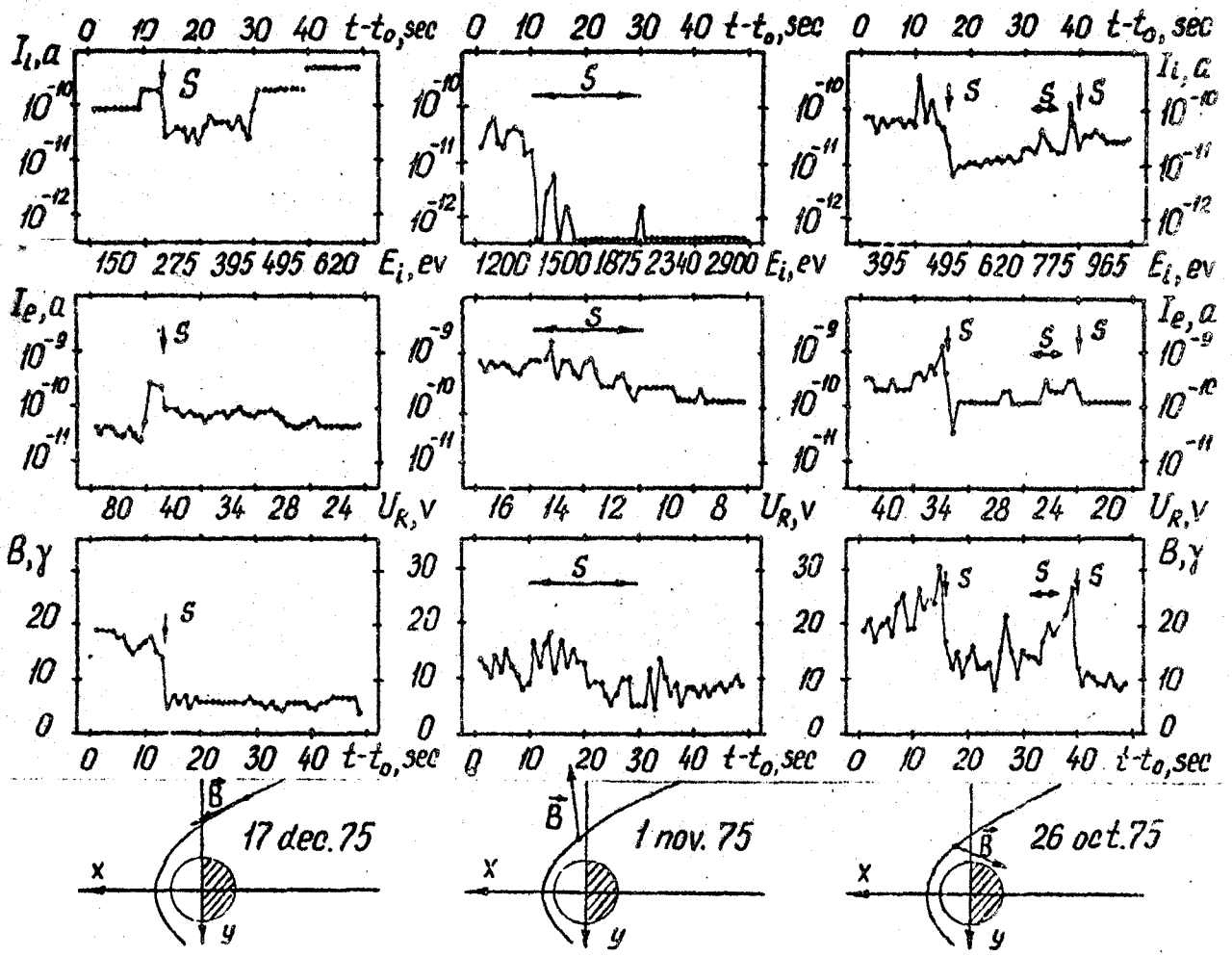
0 10 20 30 40 t-t₀, sec
I_i, a
10^-10
10^-11
10^-12
S
150 275 395 495 620 E_i, ev
1200 1500 1875 2340 2900 E_i, ev
395 495 620 775 965 E_i, ev
I_e, a
10^-9
10^-10
10^-11
80 40 34 28 24 U_K, V
16 14 12 10 8 U_R, V
40 34 28 24 20 U_R, V
B, γ
30
20
10
0
17 dec. 75
1 nov. 75
26 oct. 75
B
x
y

Fig. 1

It should also be mentioned that some traverses showed quite a broad bow shock front where transition from the electron and ion spectra typical of the solar wind to those typical of the transition region occured along orbit sections, δ, about 1000 to 3000 km long. Fig.2 illustrates orbit sections at which satellites were intersecting bow shocks fronts. It is done in X, $\sqrt{Y^2+Z^2}$ coordinates (the X-axis is through the center of the planet and directed towards the Sun) for 33 orbits of Venera-9 and Venera-10 satellites. According to the Figure it can be assessed that a fairly broad bow shock was recorded in 30% cases.

The values of bow shock thickness observed near Venus can be so much different (from $\delta \lesssim 10$ km to $\delta \approx 3000$ km) owing to different types of shock wave structures, depending on Mach numbers, ratios of thermal to magnetic field energies on θ-angle between the magnetic vector and the vector of the normal to the bow shock, etc. For large Mach numbers typical of a near-Venus bow shock the most essential parameter is θ. As is known, transition from the plasma state before the shock front to that behind it at $50° \lesssim \theta \lesssim 90°$ occurs at distances $c/\omega_{pe} \lesssim \delta \lesssim 10\, c/\omega_{pi}$ (greater δ correspond to smaller θ) which, if ion concentration in the solar wind is $0.5 \lesssim n_i \lesssim 20$ cm^{-3}, results in 1 km $\lesssim \delta \lesssim$ 3000 km [9]. For smaller θ the thickness of a pulsating front can reach about 12000 km [9].

Since Venera-9 and Venera-10 satellites intersect the near-planet bow shock not far from the ecliptic and since, as a rule, the interplanetary magnetic field component perpendicular to the ecliptic is small, the θ-angle value for any particular bow shock intersection can be evaluated by the angle between the projections of $\vec{B}$-vector on the ecliptic (which

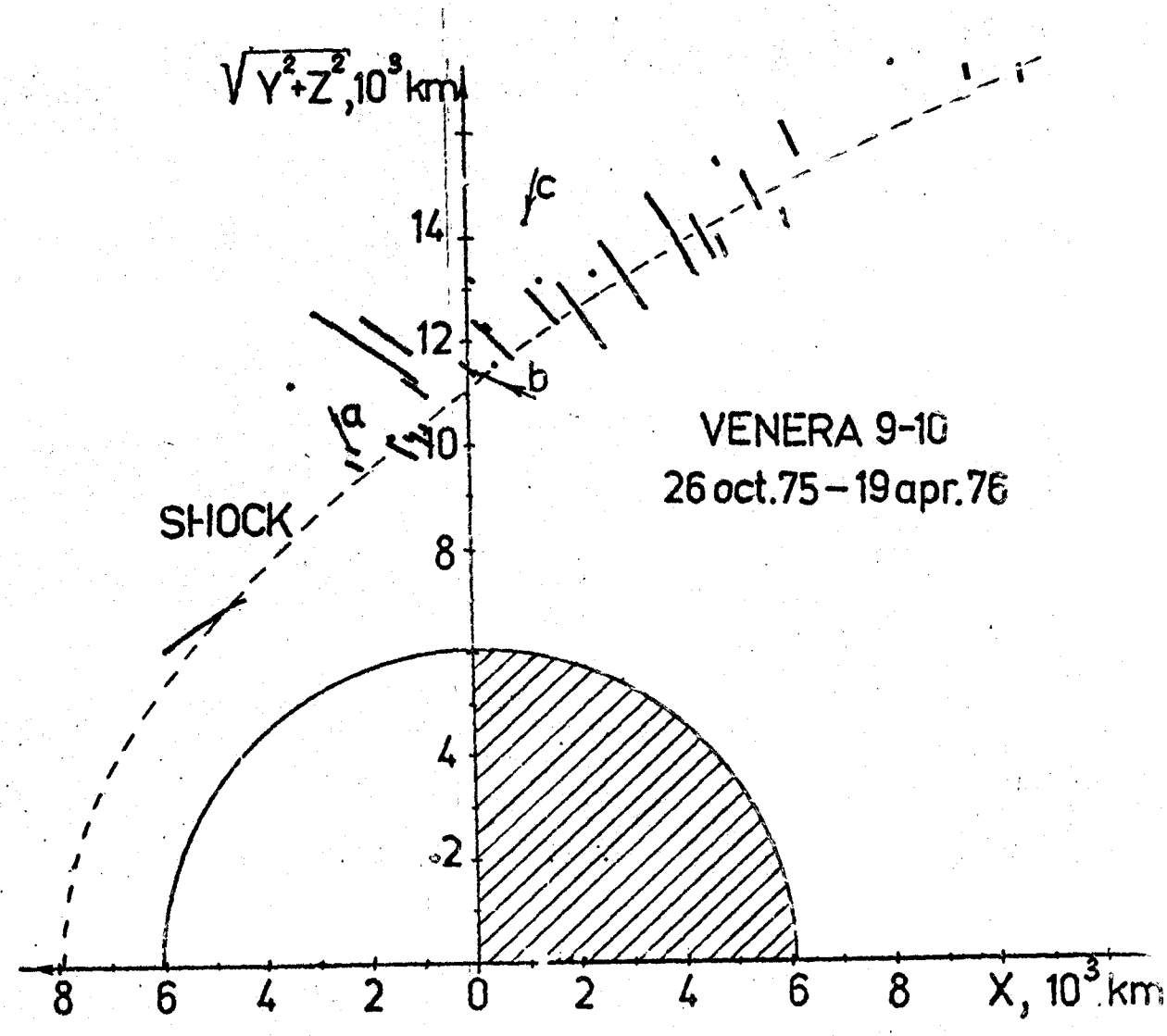
$\sqrt{Y^2+Z^2}$, 10^3 km
14
12
10
8
4
2
a
b
c
SHOCK
VENERA 9-10
26 oct.75 – 19 apr.76
8
6
4
2
0
2
4
6
8
X, 10^3 km

Fig. 2

are given in the bottom of Fig.1) and the normal to the bow shock.

As is seen from Fig.1, θ is close to 90° on December 17, but it considerably differs from this value on November 1 and October 26. The expected bow shock thickness during these dates' orbits is $\delta \approx c/\omega_{pe} \approx$ 2 km and $\delta \approx c/\omega_{pi} \approx$ 30 and 60 km, respectively (n_i measurements were used after the satellite entered the solar wind), it is in reasonable agreement with the above estimates of bow shock thickness during these passes. The examples given and the totality of all bow shock intersections near Venus allow a conclusion to be made about the dependence of bow shock structure on the angle between $\vec{B}$-vector and the normal to the front, similar to that for a near-Earth bow shock (see e.g. [9]): bow shock thickness grows with dimishing θ ; it sometimes reaches up to about 3000 km far small θ . Previously the dependence of the near-Venus shock front structure on θ was mentioned according to the data of two bow shock intersections by Mariner 5, when it entered the transition region when it left it [10] .

According to Fig.2 the spread of the points where the satellites intersected the shock front, observed on different orbits is rather small; the bow shock positions corresponding to these points group near those closed to the planet. This typical feature of near-Venus bow shock already mentioned in [6,7] from smaller number of intersection is the evidence to the stable size of an obstacle which creates a near-Venus bow shock. The dotted line in Fig.2 (as in figures that follow with the position of the bow shock) shows the position of the bow shock, calculated in [11] for an obstcale characterize by parameter $H/r_0 \approx .01$ and the height of a stagnation point over

the Venus surface ~500 km. Only in 6 orbits out of 33 the intersection of bow shock was recorded at distances exceeding 1000 km from the front given in Fig2.

The stability of an obstacle is also confirmed by the absence of relationship between the dynamic pressure of the solar wind, ρV^2 and the bow shock position. In fact, for three bow shock intersections marked by arrows in Fig.2 solar wind ρV^2 was equal to (a) $1.4 \cdot 10^{-8}$ dyn.cm^{-2}, (b) $4.2 \cdot 10^{-8}$dyn.cm^{-2} (c) $8.4 \cdot 10^{-8}$dyn.cm^{-2} respectively, while the distance of the bow shock from the planet remained practically the same for (a) and (b) intersections and grew (with growing ρV^2) for (c) intersection. By way of comparison it should be mentioned that the location of the shock front near the Earth and Mars is ρV^2 - dependent and its distance from the planet decreases with growing ρV^2 [12,13] .

It seems that a bow shock always present near Venus and its accurately determined spatial location make it possible to give up some of the earlier proposed hypotheses about solar wind interaction with Venus. These are the model [14] according to which a bow shock cannot exist near Venus and the assumption [15] about a possibility of an attached bow shock near Venus (see Fig.2).

III. Electron component in the plasma flow-around zone and in the optical umbra of the planet

Fig.3 illustrates electron spectra obtained on board Venera-9 on November 11, 1975, in the solar wind, transition region and in the corpuscular umbra region (characterized by

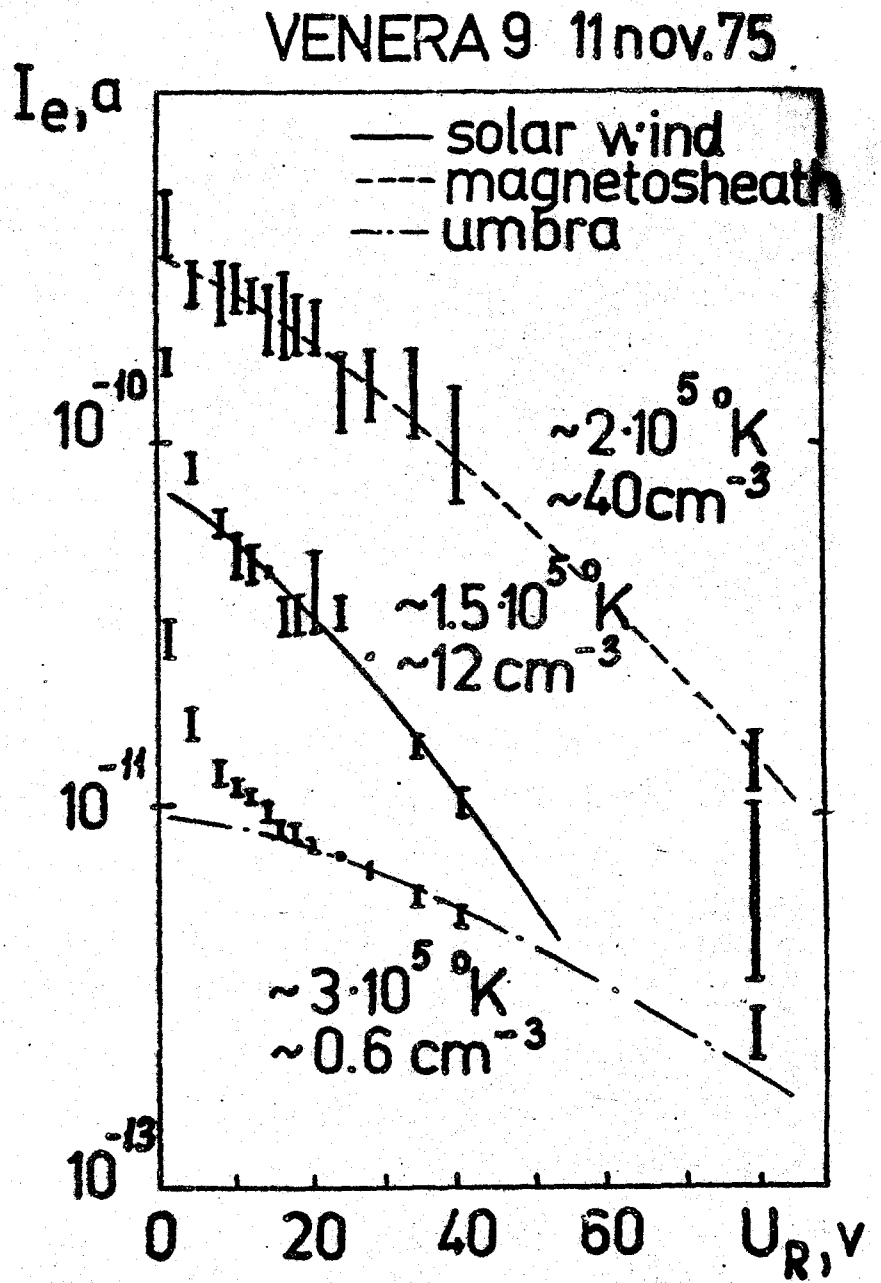
VENERA 9 11 nov. 75
I_e, a
solar wind
magnetosheath
umbra
10^{-10}
10^{-11}
10^{-13}
~2·10^5 °K
~40 cm^{-3}
~1.5·10^5 °K
~12 cm^{-3}
~3·10^5 °K
~0.6 cm^{-3}
0
20
40
60
U_R, V

Fig. 3

the absence of clearly defind ion fluxes directed from the Sum [6.7] . In Fig.3 vertical lines show within which limits currents I_e recorded by an electron analyzer with the fixed value U_R varied during 10 sec. As this figure shows during the motion from the solar wind to the transition region electron fluxes (proportional to I_e) increase at all values U_R; fluctuations of recorded electron fluxes considerably increase. The least electron fluxes are recorded in the region of the Venus corpuscular umbra. In this zone electron flux fluctuations are considerably less than electron flux fluctuations in the transition region.

One can judge on the fluctuation value of charged particle fluxes in the transition region by the given in Fig.4 results of ion fluxes ($\sim I_i$) measurements in energy interval $2080 \leq E_i \leq 2600$ eV and electron fluxes ($\sim I_e$) with energy $E_e \geq 10$ eV. As Fig.4 illustrates in the transition region $\Delta I_i/I_i \sim \Delta I_e/I_e \sim 1$, therefore, under the conditions of strongly fluctuated charged particles fluxes the fluctuation level should be taken into account for the adequate description of plasma state. To determine the parameters of charged particle distribution function we minimized the average square deviation of calculated values of currents of I_i and I_e from the measured values. Such a method makes it possible to obtain reliable numeral results only for plasma states with a low fluctuation level and a distribution function close to Maxwellian one.

Another peculiarity of measurements of electron and ion plasma components in the Venus neighbourhood on Venera-9 and Venera-10 is the fact that systematic variation of plasma concentration during the time of one spectrum measurement should be taken into account. For the most passes in the transition region n_e variation is typical in 2 times for 160 sec and during

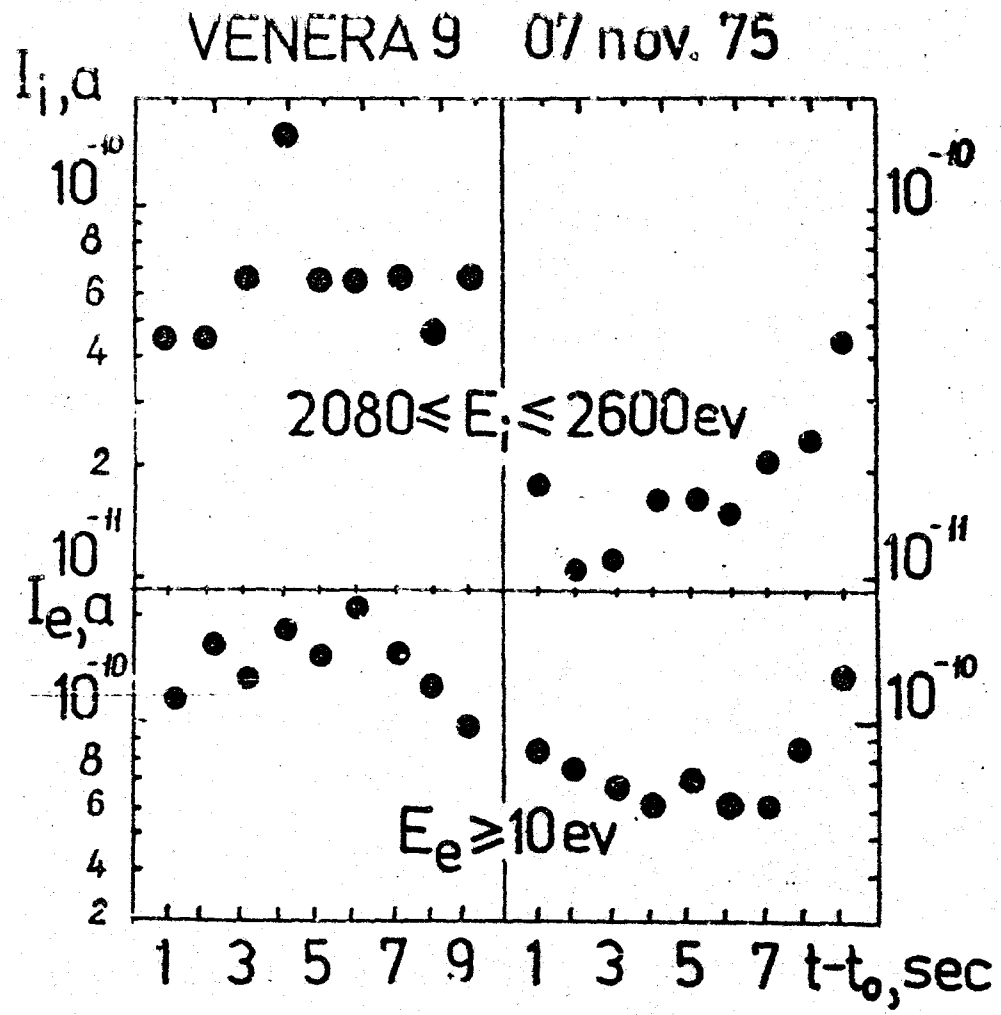
VENERA 9 07 nov. 75
I_i,a
10^{-10}
8
6
4
2
10^{-11}
$2080 \leqslant E_i \leqslant 2600$ ev
I_e,a
10^{-10}
8
6
4
2
$E_e \geqslant 10$ ev
1 3 5 7 9 1 3 5 7 $t-t_o$,sec

Fig. 4

the processing it leads to the temperature decrease and electron concentration increase.

In Fig.3 smooth curves demonstrate electron spectra corresponding to experimental values I_e and calculated for given in Figure values n_e and T_e with electron transport velocity equal to ion transport velocity V_i in the transition region, in the solar wind and with the transport velocity equal to zero (isotropic distribution) in the corpuscular umbra region. As Fig.3 shows during the motion from the solar wind to the transition region electron concentration and temperature increase. During the moving from the transition region into the corpuscular umbra electron concentration sufficiently decreases and T_e slightly increases mainly due to slower decay of electron fluxes with high energies as compared to quicker decay of electron fluxes with low energier (see Fig.3).

One of the peculiarities revealed during the measurements of electrons on board Mariner 10 is the depletion of electron plasma component by the particles with energy of several hundreds of electron-Volts [16] observed in several parts of the transition region behind bow shock. According to [16] this effect could appear during the interaction of electrons with mentioned energies and the planet atmosphere, and it was observed in the magnetic field tubes passing through the Venus atmosphere. The analyses of the results measurement of electron with energy $I_e \geq 150$ eV on Venera-9 and Venera-10 showed that in some cases in the transition region there was observed the depletion by energetic electrons as on Mariner 10 [16] . However in other cases with the approximately same orientation of local magnetic field this depletion was not observed. As an example Fig.5 demonstrates the measurements of electrons with

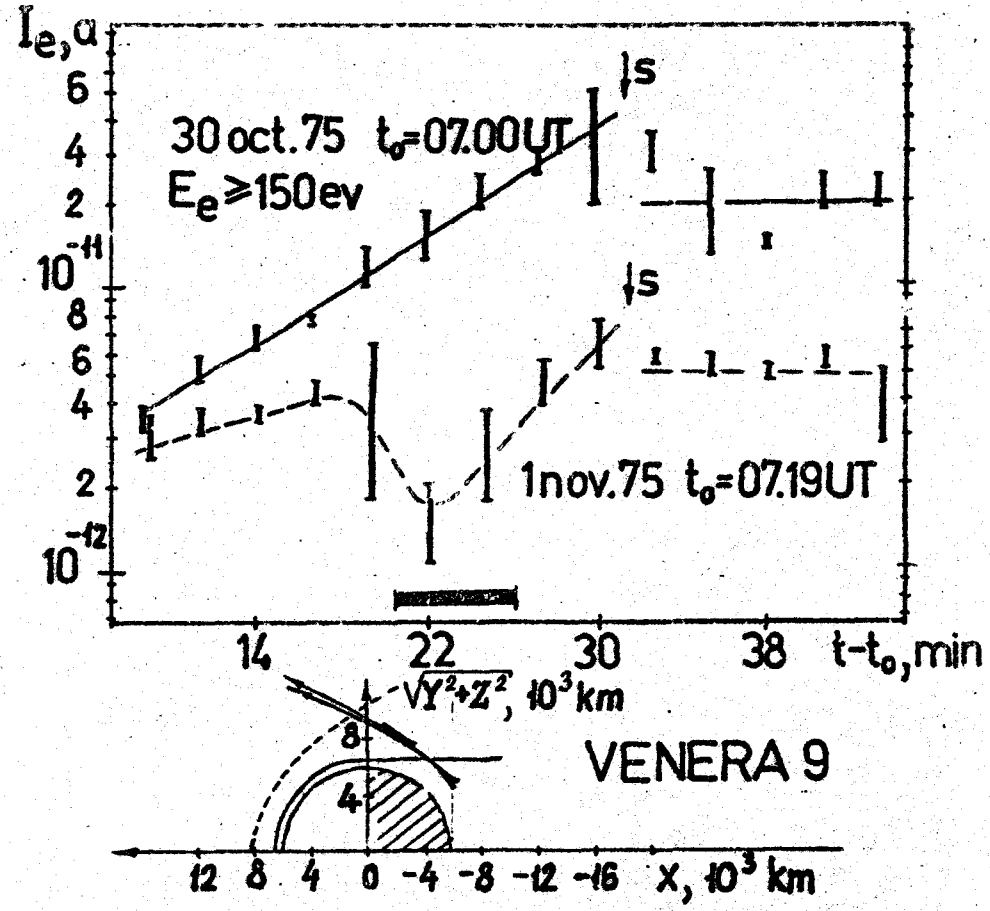
I_e, a
6
4
2
10^{-11}
8
6
4
2
10^{-12}
30 oct.75 t_o=07.00UT
$E_e \geq 150$ev
1nov.75 t_o=07.19UT
14
22
30
38
t-t_o, min
$\sqrt{Y^2+Z^2}$, 10^3 km
8
4
VENERA 9
12 8 4 0 -4 -8 -12 -16 X, 10^3 km

Fig. 5

energies $E_e \geq 150$ eV made on Venera-9 on October, 30 and November 1, 1975. During these days electron fluxes with energies $E_e \geq 10$ eV grow monotonically with the satellite orbital motion (see Fig.3, below). The magnetic field orientation in the solar wind and on t-axis, marked by a thick line and in the orbit section where the depletion by energetic electrons was observed on the 1st of November, is approximately the same. However, on the 30st of October the depletion was not observed. Therefore on the basis of Venera-9 and 10 data it is difficult to judge on the origin of considered effect and on the correctness of explanation given in [16] .

Using the some measurements of electron plasma component on Venera-9 and Venera-10 made in cases with approximately the same solar wind velocities ($310 \leq V_i \leq 360$ km/sec) the distribution of electron fluxes and concentrations in the region of interaction of the solar wind with Venus can be plotted. In Fig.6 for four passes of Venera-9 and one pass of Venera-10 position of the satellites are shown by various marks on their orbits when the recorded electrons with energy $E_e \geq 10$ eV in 2; 1; 0.5; 0.25; 0.12 times differ from electron fluxes with $E_e \geq 10$ eV in the solar wind for each pass. In this case, in Fig.6 thick lines connecting the same marks show the surface on which the ratio between electron fluxes with energy ≥ 10 eV and the flux in the solar wind is constant.

Electron temperature T_e in the considered passes always exceeds 10 eV. When Fig.6 was plotted electron flux values with energy ≥ 10 eV was used; in this case the fraction of electron fluxes with energy ≤ 10 eV, which was not taken into account, refers to the part of distribution function, which at $T_e > 10$ eV can be neglected while determining full electron flux. Electron

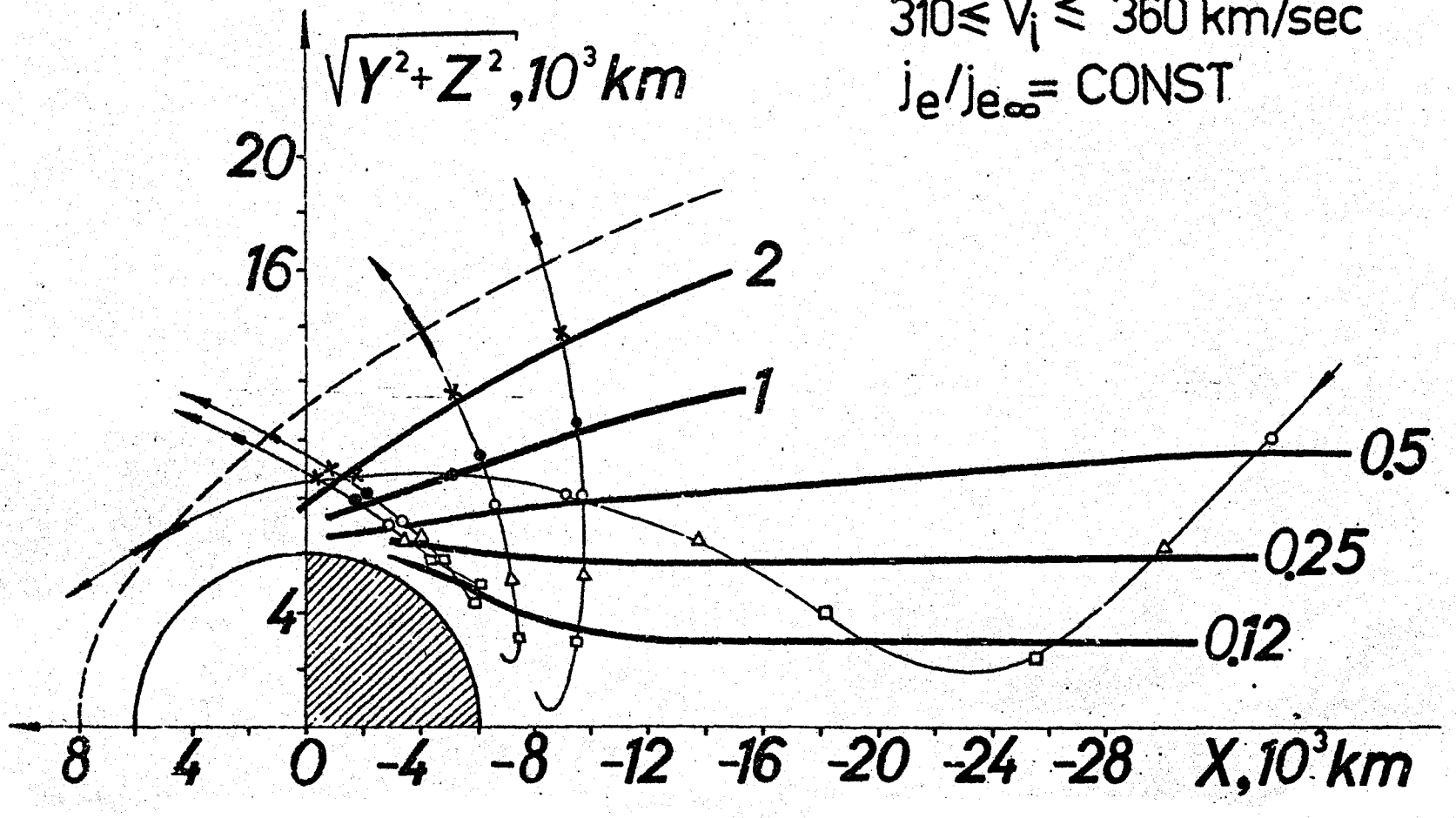
$\sqrt{Y^2+Z^2}, 10^3$ km
310≤ V_i ≤ 360 km/sec
$j_e/j_{e\infty}$ = CONST
20
16
4
2
1
0.5
0.25
0.12
8
4
0
-4
-8
-12
-16
-20
-24
-28
X, 10^3 km

Fig. 6

thermal velocity is much more than bulk one and in this case the measured flux is proportional to the omnidirectional electron flux. Fig.7 illustrates the distribution of electron concentration for the same passes in the region of solar wind interaction with Venus (in relative units $n_e / n_{e\infty}$; the values refering to the solar wind will be marked by ∞ like Spreiter had done [11], [17] . When passing from data on $j_e / j_{e\infty}$ (Fig.6) to data on $n_e / n_{e\infty}$ (Fig.7) in calculation it was assumed that electron distribution function is a Maxwell one while actually it differs from the the Maxwell function. During further processing it can be better approximated therefore data given in Fig.7 should be considered as preliminary data.

Antisolar ($X < 0$) part of solar wind region disturbed by Venus can be conditionally divided into three zones: external $D = \sqrt{Y^2 + Z^2} > 6500 \div 7000$ km; near internal - $D < 6500 \div 7000$ km, $X >$ - 10000 km and far internal - $D <$ 6500 ÷ 7000 km, $X <$ - 10000 km ($D \approx 6500 \div 7000$ km approximately corresponds to "ionopause" of Spreiter et al. [11]).

As Fig.6, 7 demonstrate in the external region the distribution of $j_e / j_{e\infty}$ and $n_e / n_{e\infty}$ qualitatively coincides with magneto-hydrodynamic calculations of solar wind flow around impenetrable obstacle [11,17] . In the near internal region the distribution of $j_e / j_{e\infty}$ and $n_e / n_{e\infty}$ qualitatively corresponds to the theoretical calculations carried out under the assumption of the flow around obstacle by collisionless neutral gas or plasma (without magnetic field, with Debay radius much less than the obstacle dimensions), freely expanding to the corpuscular umbra (see, for example, [18]). However in the far internal region the lines of $j_e / j_{e\infty}$ =const, $n_e / n_{e\infty}$ =const are very stretched; it suggests that there should be a field, apparent-

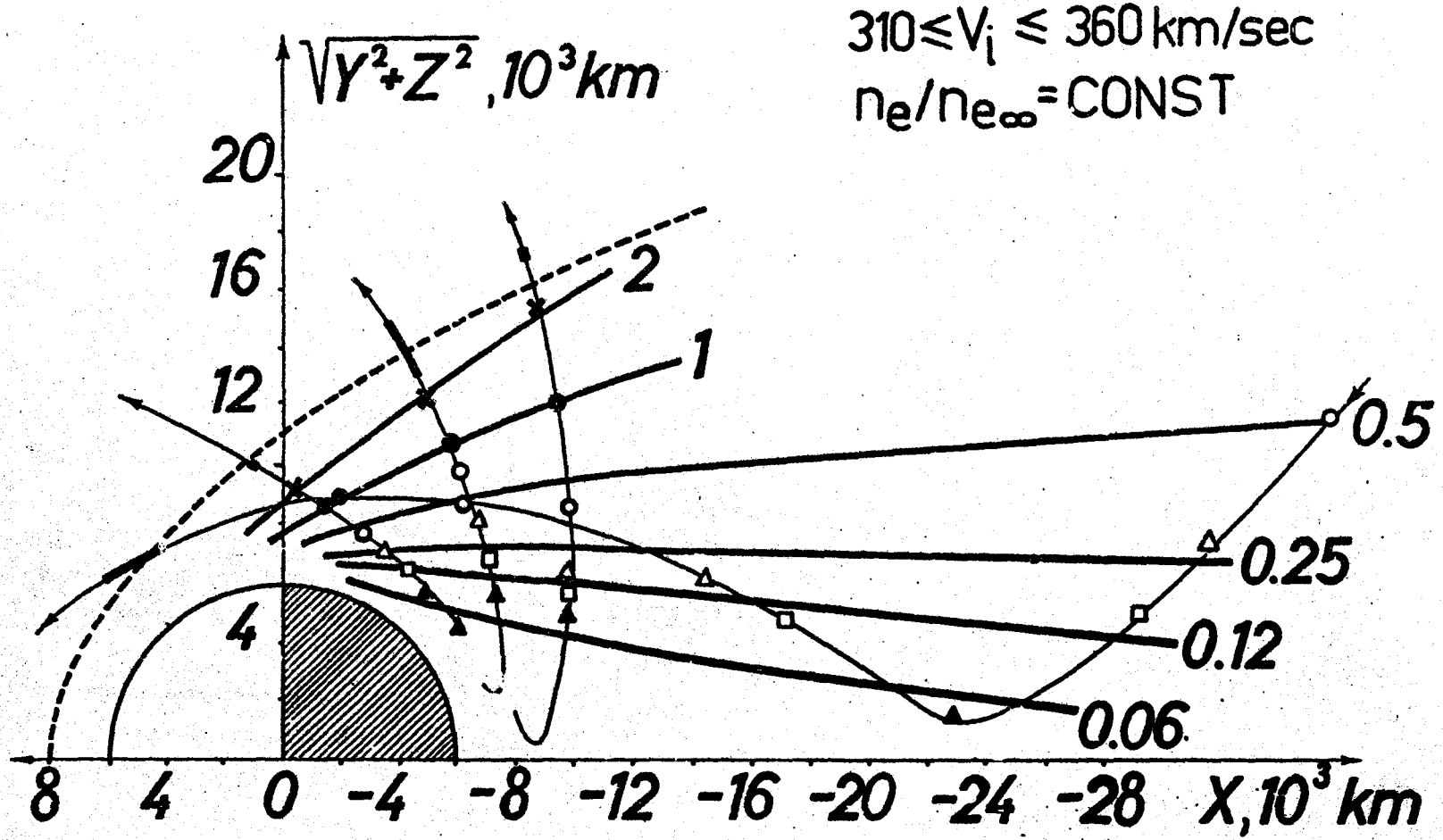
$\sqrt{Y^2+Z^2}$, 10^3 km
$310 \leq V_i \leq 360$ km/sec
$n_e/n_{e\infty}$ = CONST
20
16
12
4
2
1
0.5
0.25
0.12
0.06
8 4 0 -4 -8 -12 -16 -20 -24 -28 X, 10^3 km

Fig. 7

by a magnetic field, preventing plasma from filling the region behind the obsctacle and supporting plasma disturbance at considerable distances ($\geq$ 5 + 6 Venus radii) from the obstacle. It corresponds to the observations made by Dolginov and others [19] who recorded the magnetic field with $B_x > B_{y,z}$ at high X.

Extended curves (Fig.6,7) of $j_e / j_{e\infty}$ =const and $n_e / n_{e\infty}$ =const which are lower than $D \approx 8000$km converge at the planet terminator at the height of about 500+1000 km close to the height of the obstacle, deflecting the solar wind, estimated in [6,7] from the data of ion measurements (see, also, section IV).

The results of calculations carried out by Spreiter's group [11,17] are the only results giving a "global" picture of the solar wind flow around the planet (including the fields of plasma concentrations, its bulk velocities and magnetic field); they are a convenient "frame of reference", with which plasma characteristics in the solar wind zone disturbed by the planet can be compared.

IV. Ion plasma component in the flow-around zone in the Venus optical umbra

The analysis of ion measurements makes it possible to reveal besides the transition region, the regions of corpuscular umbra and penumbra [6,7] . These regions were determined phenomenologically. The region was called a corpuscular umbra where there was no regular registration of ion fluxes by Faraday cup, only separate ion flux spikes distributed in all energy intervals in disorder, were observed. The region was called a penumbra where lower (in comparison with the transi-

tion region) ion fluxes with lower antisolar velocity V_i were recorded.

According to Spreiter's calculations [11,17] $V_i/V_{i\infty}$ in the region X < 0 everywhere > 0.75; let us take the condition $V_i/V_{i\infty} \leq 0.75$ for the determination of the corpuscular penumbra.

Fig.8 illustrate ion spectra obtained from Venera 9, I.XI.1975 and Venera 10, 19.IV.1976. These two days are characterized by fairly low values of the solar wind velocity (310 km/sec and 350 km/sec respectively), T_i ($6.5 \cdot 10^4$°K and $9 \cdot 10^4$°K) and by high values of n_i (35 cm^{-3} and 65 cm^{-3}). It should be mentioned that on the 19th, IV, 1976 in the solar wind, ion spectra had an anomal "tail" in the region of high energies (2÷4 keV). In the figure each ion energy spectrum corresponds to the orbit section with which it is connected by a straight line; each spectrum has calculated plasma parameters. In both cases the solar wind characteristics during the satellite movement in the region disturbed by the planet almost did not change.

As Fig.8 shows on the 1st of November during the satellite pass from the solar wind into the region of its interaction with Venus, plasma parameters changed in the following way: at bow shock bulk velocity V_i decreased and temperature T_i and ion concentration n_i increased; with further deepening into the transition region V_i was practically constant, and n_i decreased from 110 to 13 cm^{-3}; the spectrum recorded in 4^h35^m UT characterized by a considerable fall of V_i (to 110 km/sec) we interpret as related to the corpuscular penumbra zone. Further spectra (their sample is given for $t=4^h27^m$ Nov.1.1975 belong to the corpuscular umbra, they are characterized by the fact that regular fluxes were not recorded at all, and in all energy

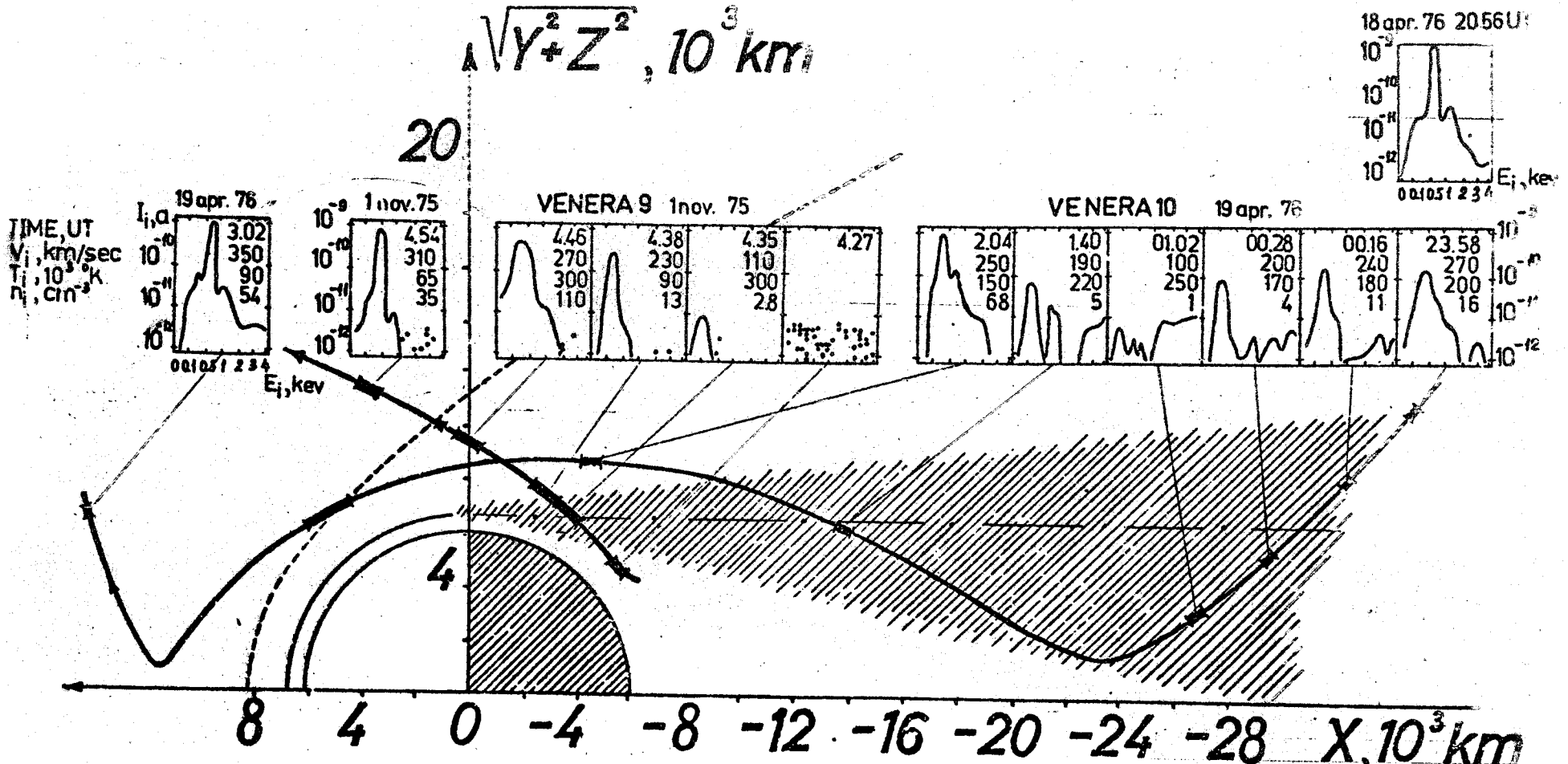
$\sqrt{Y^2+Z^2}$, 10^3 km
20
4
8 4 0 -4 -8 -12 -16 -20 -24 -28 X, 10^3 km
TIME, UT
V_i, km/sec
T_i, 10^5 °K
n_i, cm^{-3}
I_i, a
19 apr. 76
3.02
350
90
54
1 nov. 75
4.54
310
65
35
E_i, kev
VENERA 9 1 nov. 75
4.46 4.38 4.35 4.27
270 230 110
300 90 300
110 13 2.8
VENERA 10 19 apr. 76
2.04 1.40 01.02 00.28 00.16 23.58
250 190 100 200 240 270
150 220 250 170 180 200
68 5 1 4 11 16
18 apr. 76 20.56 UT
E_i, kev

Fig. 8

intervals in 30% of telemetry samples only ion spikes were observed. The results obtained in the corpuscular umbra are given in more detailes in [6,7] . There were no ions with energies $\geq$2 keV in the session of Nov.1, 1975 either in the transition region or in the corpuscular penumbra, and their registration in the corpuscular umbra indicates that there are acceleration mechanismas in this region (also see data in [6,7]).

On the section of the orbit of Venera-10, passing inside the solar wind region disturbed by the planet solar ion fluxes were regularly recorded everywhere, so this section although it passed through the planet optical umbra, was only in the transition region and in the corpuscular penumbra.

It gives an evidence that the "length" of the umbra in the case under consideration is no more than 3 to 4 R_V (from the planet) and that the planet's penumbra is in the hatched region in Figure 8. Inside the region the bulk velocity does not exceed 0,75 V_i in the undisturbed solar wind, as has already been mentioned. When a satellite passes near the planet's terminator sometimes the penumbra is beeing recorded only in one ion spectrum, which allows direct measurements of an obstacle height [6,7] .

The ion spectra measured on April 19, 1976 have several maxima recorded in different energy intervals. However, all the spectra among these maxima have one largest "major" maximum at the lowest energy E_{min}, and the ion flux magnitude and E_{min} which correspond to that maximum systematically decreased when the satellite was moving deeper from the bow shock into the transition region and into the penumbra region. Hence, there is a good reason to believe that the "major" maximum mentioned is determined by solar wind protons. The value of n_i

falls from 15 cm^{-3} down to $\lesssim$ 1 cm^{-3}, that of V_i from about 270 km s^{-1} down to $\lesssim$ 100 km s^{-1}, T_i increases by about 1,5 times from the outer boundary of the penumbra (23^h58^m UT, Apr. 18, 76) to the area deep within this region (1^h40^m UT Apr. 19, 76).

According to Dolginov et al. measurements [19] the change of magnetic field component sign was recorded at 00^h42^m UT on April 19, 1976 (antisunward $\vec{B}$ was replaced by sunward $\vec{B}$). Fig.9 shows ion spectra measured in the vicinity of Venera-10 orbit section within which $\vec{B}$ changed its sign. Intense high-energy ion fluxes were recorded at 00^h42^m UT. Their temperature can be estimated as about 10^3 eV.

Zero value of B_x (the major $\vec{B}$-component; $B_x > B_{y,z}$ in this region) corresponds to the minimum magnetic energy; so the increase of plasma pressure in this region is quite natural. On ion spectra in both sides from the place of B_x-turn an increase of the energetic ion fluxes with energies $\gtrsim$ 2 keV is observed that seems similar to a plasma-sheet in the Earth's magnetosphere tail (which as known consists of the charged particles with energies of the order of keV units).

Occurence of high energy ions near the points where B changed direction was observed in the other cases (at the lower values of X) when according to the measurements made by Dolginov et al. B_x changed its sign (for example, on Nov.11,75 and on Nov.25, 75).

Discussion

The consideration of the above mentioned data obtained near Venus with wide-angle plasma analyzers first af all proves

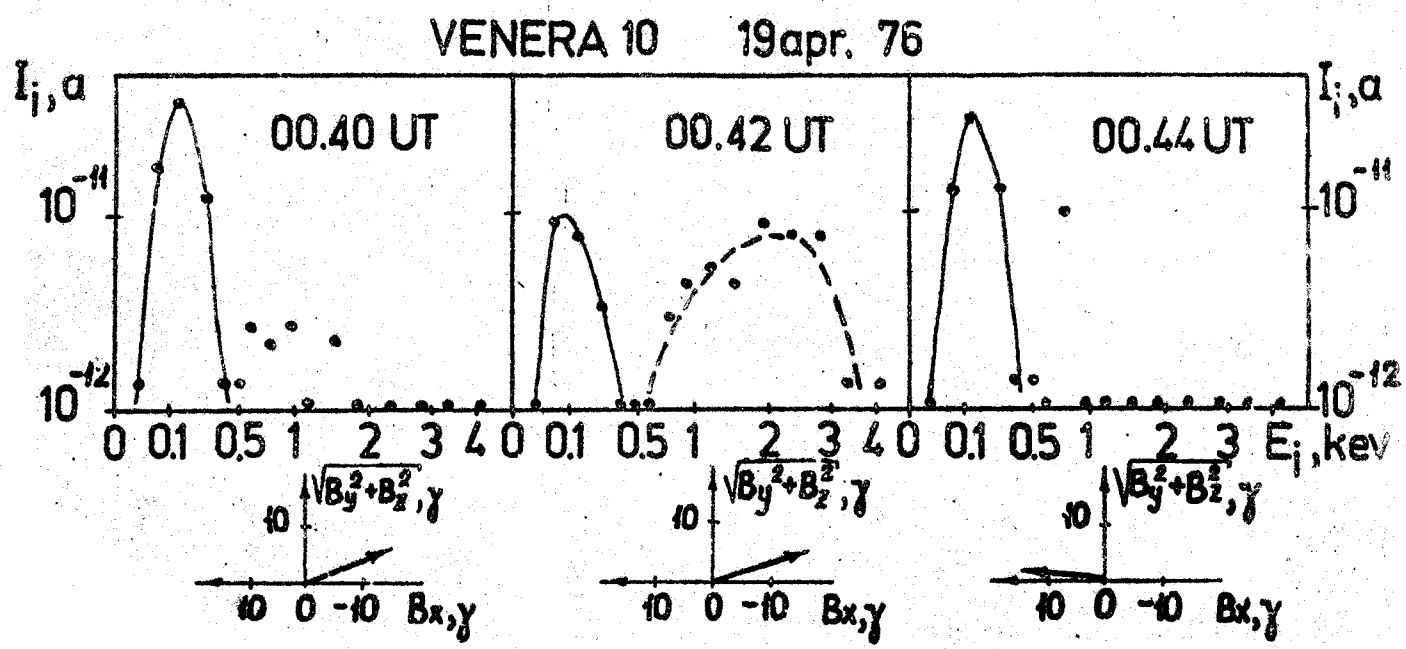
VENERA 10 19apr. 76
I_i, a
10^{-11}
10^{-12}
00.40 UT
00.42 UT
00.44 UT
0 0.1 0.5 1 2 3 4
E_i, kev
$\sqrt{B_y^2+B_z^2}$, γ
10
10 0 -10 Bx, γ

Fig. 9

that the position of the detached bow shock is described quite well by the magnetohydrodynamic calculations made by Spreiter [11] under the assumption one-fluid plasma model and the completely impenetrable obstacle (full pressure balance at the "ionopause") with M_∞ =8, $\gamma = \frac{5}{3}$ and H/r_0 =0.01 (Fig.2). Plasma density distribution in the transition region behind the bow shock with $D \geq$ 8000 km is qualitatively consistent with the calculations made by Spreiter [11,17] . Despite the fact that during the time which complies with the bow shock front crossing near Venus (Fig.2) the solar wind velocities varied in the broad intervals (300 to 800 km/sec), the bow shock position was far more stable than near the Earth or Mars [12,13]. From our viewpoint it proves that the obstacle which creates a bow shock at Venus has the other nature than that at the Earth and Mars, its sizes are sufficiently stable and slightly depend on variations in solar wind plasma parameters. The agreement between the bow shock position and the calculations [11] made under the assumption that there is no dissipation of the solar wind energy in obstacle points to the fact that this dissipation is insignificant. At the same time and the existence of such a dissipation is beyond any doubt and can be further observed. As seen from [20] the interaction between solar wind electrons occuring in the planet optical umbra with the night-side atmosphere makes an important contribution to formation of the planet night-side ionosphere. Such an interaction should take place also in the planet day-side atmosphere. However, since the data of Venera-9 and Venera-10 radio occultation observations reveal that the electron density value in the day-side maximum of ionization strongly depends on the solar zenith angle [21,22] a conclusion can be made that the solar wind con-

tribution to ionization in this case is insignificant and the ultraviolet solar radiation is the main source of ionization in the day-side ionosphere. Thus, despite the fact that the solar wind energy dissipation in the Venus atmosphere probably is present it cannot be essential.

In recent paper of Russel the data of magnetic measurement on Venera-4 are revised and a conclusion is made that the Venus surface magnetic field is ~30γ [23] . This value is a maximum from those suggested up to the present. However, the magnetic field even with such a value of B is insufficiently high for being the obstacle which deflects the solar wind at Venus. None of investigators considered the Venus magnetic field as an obstacle deflecting the solar wind near the planet.

Despite the fact that during the last ten years a series of papers dealing with the characteristics of the obstacle near Venus was published [8,11,14,15,17,23-29] no sufficient experimental data are available to solve this problem finally. The concept that the solar wind can decelerate near Venus only at ionospheric heights is common to all the papers. There were the various suggestions on the causes of deceleration (impenetrability of the ionosphere for solar wind plasma - Dessler [28] , Spreiter et al. [11] , Bauer et al. [29] , the magnetic field generated by currents induced in the ionosphere due to electric field $-\frac{1}{c}[\vec{V}_1 \times \vec{B}]$ - Johnson and Midley [26] , Cloutier and Daniell [27] , or loading of the solar wind flow by ionospheric ions - Cloutier et al. [24]), however there are no estimations of obstacle altitude in the subsolar point above ~500 km.

Since recently Russel argued in favour of the absence of the intrinsic magnetic field of the Mars [41] a comparison of some data which have been obtained from the satellites of both

planets is of interest. As known Vaisberg et al. paid great attention to the concept of the bow shock mean position suggesting that the detachments of the near Martian bow shock from the planet which have been given by Gringauz et al. [30] are too far [31] . Fig.10 gives (in units expressed in planet radii) the mean position of the bow shock near Mars that has been calculated by Vaisberg et al. [31] (the closest to the planet from all the estimates available in present) and the data on the bow shock intersections by the satellites Venera-9 and Venera-10 which have been already shown in Fig.2. It is evident that though the Venus ionosphere is fairly alike to that of Mars (see for example [32]) there is some cause of the fact that the bow shock near Mars is substancially farther from the planet than that near Venus. We believe that the intrinsic magnetic field of the planet sufficient to deflect the solar wind at Mars is the cause. Such a field is absent at Venus.

The authors of papers [11,17] who presented (as far as been mentioned) the only "global" picture of solar wind flow around the Venus, noted that actually the solar wind energy dissipation near the obstacle should cause the deceleration of plasma in some broad boundary layer. According to Spreiter [17] this dissipation can be taken into account if the "effective viscocity" is included to the magnetic hydrodynamics equation. The specific mechanisms which can produce this viscocity are reviewed in the paper by Hartle [33] . They are following: charge exchange of protons with neutrals (Wallis [14]), mass loading of the solar wind with atmospheric photo-ions, electrodynamic effects due to the currents induced in the ionosphere, plasma instabilities caused by the opposite directions of the density and temperature gradients at the solar wind ionosphere

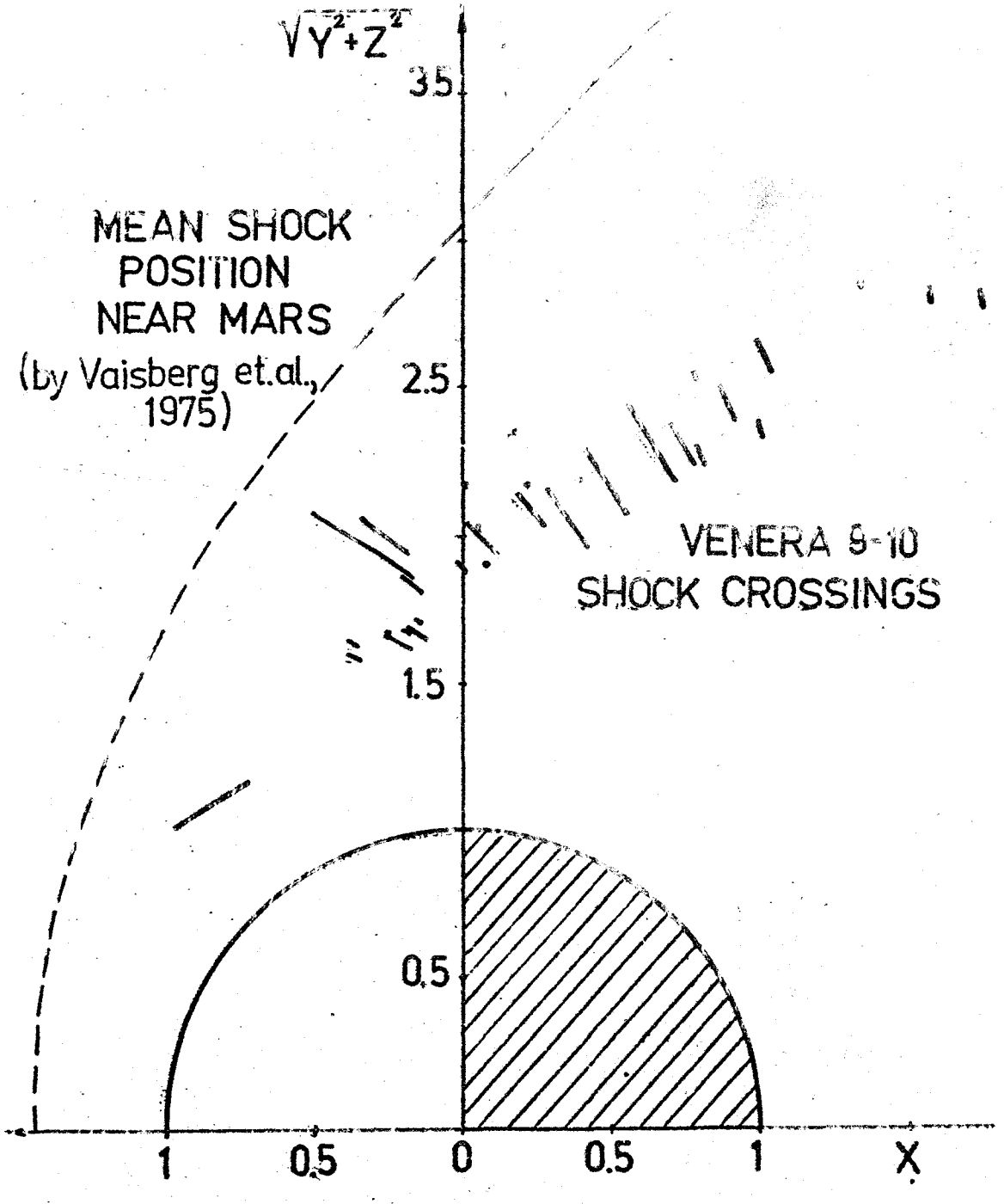
$\sqrt{Y^2+Z^2}$
3.5
2.5
1.5
0.5
MEAN SHOCK
POSITION
NEAR MARS
(by Vaisberg et.al.,
1975)
VENERA 9-10
SHOCK CROSSINGS
1
0.5
0
0.5
1
X

Fig. 10

boundary. In [33] as well as in [6,7] the probability of Kelvin-Helmholtz instability is mentioned.

In 1974 Vaisberg and Bogdanov [34] to confirm their assumption that the nature of the obstacles decelerating the solar wind near Mars and Venus are of similar nature (which from our view-point it is not correct) noted the presence of the broad boundary layer near Venus using the data of Venera-4 ion measurements (from our point of view it is correct). However, Vaisberg et al. after obtaining the results of their own ion measurements from Venera-10, while interpreting them in 1976 have not used the conception of boundary layer but spoke about a rarefaction wave [35,36] .

We consider that it is the effective obstacle viscocity that is the main cause of the penumbra region formation (see [6,7] and Figure 8), where $V_i / V_{i\infty} \leq 0.75$, i.e. lower than the value permissible by the calculations in which dissipation is not taken into account.

The results of the calculations of the boundary layer near the obstacle boundary that have been made by Tejada and Dryer for a two dimensional model [37] are qualitatively consistent with our results.

Fig.8 shows that corpuscular penumbra which begins above the planet terminator while from the planet detaching antisunward enlarges in the both directions: to bow shock and to the optical umbra.

The essential feature of an antisolar region of near Venus space is the existence inside it ($D \lesssim 7 \cdot 10^3$km) of constant plasma density lines aligned along Sun-Venus direction (Figure 7). Simultaneously, Dolginov et al. observe in the same region the magnetic field aligned along X-axis [19] . It

seems to us reasonable to call this region the Venus plasma-magnetic tail. A dash-and-dot line in Fig.8 is the approximate position of the plasma magnetic tail. A part of the corpuscular penumbra is inside the plasma-magnetic tail. The bulk velocity of plasma in this region continues to decrease while detaching from the bow shock (i.e. while deepening into the plasma-magnetic tail). In so doing variation of plasma parameters in this penumbra region reminds variation of parameters of the Earth magnetosphere tail's plasma mantle [38,39] . Hence, it cannot be excluded that this part of penumbra region is produced due to the processes close to those occuring in the Earth's plasma mantle.

The umbra region (where the ion fluxes are not reccrded regularly by Faraday cup but about in 30% of readings the ion flux spikes are recorded with energies irregularly distributed in all energy intervals) beginning above the planet terminator gradually narrows while the penumbra enlarges and probably extends to the distance $\lesssim (3 \div 4)\, R_V$. Obviously, this distance must depend on the ion bulk velocity and on the ion temperature in the transition region. The fact that the accelerated particles which are absent in the transition region can be observed in the umbra as spikes gives an evidence that the acceleration processes strongly vary in time. Perhaps they are associated with some wave-like phenomena in the plasma-magnetic tail. Ionospheric ions pick-up also results in generation of the waves which can appear in the umbra [33,40] ; However, the electron fluxes are recorded in the umbra quite regularly and the electron density is within the limits $\sim 1\ cm^{-3}$. The possible effects of the interaction of these electrons with the planet night-side neutral atmosphere are considered in [20].

The magnetic field in the umbra varies with the interplanetary field [19] .

Russel in a series of works [23,42] published in 1976-77 considering the data which have been presented by the authors of the Venera-4, Mariner-5 and Venera-9 experiments made a conclusion on the Venus magnetosphere existence due to an intrinsic magnetic field of the planet. The data in [42] give an evidence in favour of the existence of the boundary layers and the magnetic tail near Venus. Though according to our data the penumbra shape and spatial position differ appreciably from the "boundary layer" according to Russel [42] Fig.2 and the plasma-magnetic tail boundary is at much lower distances from the Sun-Venus line than in Fig.2 [42] (see our Fig.8) the data given in Fig.8 in general features do not contradict to the conclusions of [42] .

It is evidents that the plasma measurement data given in this paper do not allow to judge on the origin of the magnetic field in the plasma-magnetic tail (is it the intrinsic field of the planet or that induced by the ionosphere currents).

Aknowledgements

The authors expess their sincere thanks to A.V.Dyachkov and L.A.Shvachunova for their participation in the data processing, to T.V.Stukalova for technical assistance in preparing of this paper and to Sh.Sh.Dolginov and E.G.Yeroshenko for permission to use their magnetic field data from Venera-9, 10 satellites.

REFERENCES

1. K.I.Gringauz, V.V.Bezrukikh, L.S.Musatov, T.K.Breus, Kosmicheskie Issledovanija, 6, 411, 1968.
2. H.S.Bridge, A.J.Lazarus, C.W.Snyder et al., Science, 158, 1969, 1967.
3. K.I.Gringauz, V.V.Bezrukikh, G.I.Volkov, L.S.Musatov, T.K.Breus, Kosmicheskie Issledovanija, 8, 431, 1970.
4. H.S.Bridge, A.J.Lazarus, J.D.Scudder et al., Science, 183, 1293, 1974.
5. K.I.Gringauz, V.V.Bezrukikh, G.I.Volkov et al., Kosmicheskie Issledovanija, 12, 430, 1974.
6. K.I.Gringauz, V.V.Bezrukikh, T.K.Breus et al., Kosmicheskie Issledovanija, 14, 839, 1976.
7. K.I.Gringauz, V.V.Bezrukikh, T.K.Breus et al., in "Physics of Solar Planetary Environments", Boulder, Colorado, 1976.
8. S.J.Bauer, L.H.Brace, D.M.Hunten et al., "The Venus ionosphere and solar wind interaction", submitted to Space Sci. Rev.
9. E.W.Greenstadt, in "Magnetospheric particles and fields", ed. by B.M.McCormac, D.Reidel, Dordrecht-Holland, 1976.
10. E.W.Greenstadt, Cosmic Electrodynamics, 1, 380, 1970.
11. L.R.Spreiter, A.H.Summers, A.W.Rizzi, Planet.Sci., 18, 1281. 1970.
12. J.H.Binsack, V.M.Vasyliunas, J.Geophys.Res., 73, 429, 1968.
13. K.I.Gringauz, V.V.Bezrukikh, M.I.Verigin, A.P.Remizov, J.Geophys.Res., 81, 3349, 1976.
14. M.K.Wallis, Cosmic Electrodynamics, 3, 45, 1972.
15. C.T.Russel, J.Geophys.Res., 82, 625, 1977.
16. H.S.Bridge et al., in "Solar-Wind interaction with the planets Mercury, Venus and Mars" ed. by N.F.Ness, NASA SP-397, Washington, 1976.
17. J.K.Spreiter in "Solar wind interaction with the planets Mercury, Venus and Mars" ed. by N.F.Ness, NASA SP-397, Washington, 1976.
18. A.V.Gurevich, L.P.Pitaevskii, V.V.Smirnova, Uspekhi fizicheskikh nauk, 99, 3, 1969.
19. Sh.Sh.Dolginov et al. "Magnetic fields in the close vicinity of Venus according to the Venera-9 and Venera-10 data", to be submitted to Symposium SIV-3 IAGA, Seattle, 1977.

20. K.I.Gringauz, M.I.Verigin, T.K.Breus, T.Gombosi, "The interaction of the solar wind electrons in the optical umbra of Venus with the planetary atmosphere- the origin of the nighttime ionosphere", to be submitted to Symposium SIV-3 IAGA, Seattle, 1977.
21. Yu.N.Aleksandrov et al., Kosmicheskie Issledovanija, 14, 819, 1976.
22. O.I.Jakovlev et al., Kosmicheskie Issledovanija, 14, 722, 1976.
23. C.T.Russel, Geophys.Res.Letters, 3, 125, 1976.
24. P.A.Cloutier, M.B.McEleroy, F.C.Michel, J.Geophys.Res., 74, 6215, 1969.
25. F.C.Michel, Rev.of Geophys.and Space Phys., 9, 427. 1971.
26. F.S.Johnson, J.E.Midgley, Space Res., 9, 761, 1969.
27. P.A.Cloutier, R.E.Daniell, Jr., Planet.Space Sci., 21, 463, 1973.
28. A.J.Dessler, in "The Atmospheres of Venus and Mars", ed. by J.C.Brandt, M.B.McElroy, Gordon and Breach, New York, 1968, p.241.
29. S.J.Bauer, R.E.Hartle, J.R.Herman, Nature, 225, 533, 1970
30. K.I.Gringauz et al., Kosmicheskie Issledovanija, 12, 585, 1974.
31. O.L.Vaisberg in "Physicks of solar planetary environments", ed. by D.J.Williams, AGU, 1976, p.854.
32. K.I.Gringauz, T.K.Breus in Hundbuch der Physick, Springer-Verlag, Berlin-Heidelberg, 1976, p.351.
33. R.E.Hartle in "Physics of solar planetary environments", ed. by D.J.Williams, AGU, 1976, p.989.
34. O.L.Vaisberg, A.V.Bogdanov, Kosmicheskie Issledovanija, 12, 279, 1974.
35. O.L.Vaisberg et al., in "Physics of solar planetary environments", ed. by D.J.Williams, AGU, 1976, p.904.
36. O.L.Vaisberg et al., Kosmicheskie Issledovanija, 14, 827, 1976.
37. H.P.Tejada, M.Dryer, J.Geophys.Res., 81, 2023, 1976.
38. S.I.Akasofu, E.W.Hones,Jr., S.J.Bame et al., J.Geophys. Res., 78, 7257, 1973.
39. H.Rosenbauer, H.Grunwald, M.D.Montgomery, J.Geophys.Res., 80, 2723, 1973.

40. M.K.Wallis, Nature, 233, 23, 1971.
41. C.T.Russel, The interaction of solar wind with Mars, Venus and Mercury, Preprint Institute of Geophysics and Planetary Physics, University of California, Los Angeles, May, 1977.
42. C.T.Russel, Geophys.Res.Letters, 3, 589, 1976.

©
055(02)2 Отпечатано в ИКИ АН СССР
Т-15020 Подписано к печати 8.08.77
Заказ 1275 Тираж 150 Объем 1,5 уч.-изд.л.